# Experimental studies on the shape and path of small air bubbles rising in clean water

Mingming Wu and Morteza Gharib

## Additional information on Phys. Fluids

# Experimental studies on the shape and path of small air bubbles rising in clean water

Mingming Wu[a)]
*Department of Physics, Occidental College, Los Angeles, California 90041*

Morteza Gharib
*Graduate Aeronautical Laboratories, California Institute of Technology, Pasadena, California 91125*

This Letter reports experiments on the shape and path of air bubbles (diameter range 0.1–0.2 cm) rising in clean water. We find that bubbles in this diameter range have two steady shapes, a sphere and an ellipsoid, depending on the size of the capillary tube from which they detach. The spherical bubbles move significantly slower than the ellipsoidal ones of equivalent volume. Bubbles with diameter less than about 0.15 cm rise rectilinearly. The larger spherical bubbles follow zigzag paths while the larger ellipsoidal bubbles follow spiral paths. © *2002 American Institute of Physics.* [DOI: 10.1063/1.1485767]

The study of the motion of air bubbles rising in various fluids has been the subject of a large amount of work during the last century (see Clift, Grace, and Weber,[1] and a recent review article by Magnaudet and Eames[2]). The problem attracts much attention because it represents an important class of free boundary problem in fluid dynamics,[3] and its basic understanding is essential for the study of two phase flows that are of increasing importance in numerous industrial processes. It is known that bubbles in the diameter range of 0.1–0.2 cm rising in clean water are ellipsoidal in shape.[1,4] The bubble path is straight when the equivalent diameter is less than about 0.13–0.18 cm, but becomes either spiral or zigzag for larger bubbles.[4–9] Both spiralling and zigzagging bubbles in this diameter regime have been reported; however, various experiments are not in agreement whether the bubble spirals or zigzags when the bubble diameter exceeds a threshold. For instance, Saffman[7] observed only zigzagging bubbles using filtered water,[7] while Miyagi[5] and Aybers and Tapucu[9] observed only spiralling bubbles in the bubble diameter regime $d<0.2$ cm. The current investigation revisits this intriguing problem in a narrow parameter regime (near and above the path instability point) using modern imaging systems.

The main part of the experimental apparatus is a Plexiglas water tank with dimensions of 15 cm×15 cm×61 cm, which is large enough to neglect the wall effects.[6] At the center of the bottom plate, a specially designed fitting is mounted for the insertion of a glass capillary tube (Clay Adams), from which bubbles are released into the water tank. The bubble generation method used in our experiments is similar to the one used by Saffman[7] and Duineveld.[4] To differentiate it from other generation methods, we name it the gentle-push method. The bubble generation apparatus consists of a straight glass capillary, an L-shaped Teflon capil-

lary (0.15 cm diameter, 0.8 cm total length) embedded in a 3-port valve (Hamilton, HV Plug), and two glass syringes (see Fig. 1). Both syringe A and B are controlled by two syringe pumps (Microlab 501A from Hamilton and PHD 2000 from Harvard Apparatus). All the components are filled with water except for syringe A prior to experiments. To generate a bubble, a desired volume of air is first released into the L-shape capillary as shown in Fig. 1 using syringe A. Second, the L-shape capillary is rotated 90° clockwise from the position shown in Fig. 1 and the air bubble is gently pushed out through the straight capillary and into the water tank using syringe B. For reproducible experimental results, it is important that syringe B is operated at a slow rate of 2 $\mu$l/min or less to ensure that bubbles are released into the water quasistatically.

The bubble images are recorded by a high speed camera (1000 fps, Kodak Ektapro Motion Analyzer, Model 1000 HRC) together with a 90 mm Macro lens. The camera typically takes an image of 512×384 pixels with a viewing window of 1.84 cm×1.38 cm, in which the lower bound is ~2.0 cm above the capillary tip. The contours of the bubble images are located using MATLAB (Mathworks Inc.). The long axis $a$ and the short axis $b$ of the bubble are obtained using a Fourier transform method described in Ref. 4 by Duineveld ($N=6$ is used in our analysis). The diameter of the bubble is calculated using $d\equiv(a^2b)^{1/3}$. The resolution for the diameter measurement is ±0.001 cm.

The bubble trajectories are recorded by a specially designed three-dimensional (3D) imaging system, which is mounted on the top of the water tank. The camera maps out the $(x,y,z)$ coordinates of the bubble, where $x$ and $y$ are lateral positions of the bubble, and $z$ is the vertical distance above the needle. Here, $z$ is obtained using a quantitative defocusing mechanism.[10] A typical viewing window of the 3D imaging system is 1.5 cm×1.5 cm×20 cm, in which the lower bound is at least ~20 cm (or ~100$d$, $d$ is the bubble diameter) above the capillary tip. The imaging system is de-

---

[a)]Author to whom correspondence should be addressed. Electronic mail: mingming@oxy.edu
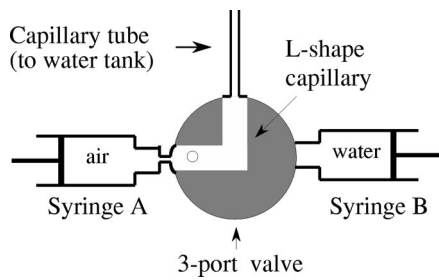
FIG. 1. Schematics for the bubble generation method.



FIG. 2. (a) Vertical terminal velocity $U$ versus diameter $d$. (b) Aspect ratio $\chi$ versus Weber number We. Scattered data points are from present investigation. Solid lines are results from Duineveld (Ref. 4), dashed lines are results from analytical calculation of Moore (Ref. 14).

signed in such a way that the spatial resolution in the $x-y$ plane is about 40 times higher than the resolution along the $z$ direction, making it an ideal instrument for recording trajectories with small lateral movements. In the current setting, the lateral spatial resolution is 0.005–0.01 cm and the vertical resolution is 0.02–0.4 cm, where the resolution varies with the distance between the bubble and the camera.

When a bubble is released into the water tank, both the high speed camera and the 3D imaging system are triggered simultaneously. For a typical experimental run, a sequence of 1000 images are recorded in one second by the high speed camera, in which two in the middle of the viewing window are used for shape and size measurements. The 3D imaging system records a sequence of 60 images in one second, from which only those within the viewing window of the camera (typically more than 45 data points) are used to obtain the bubble trajectory $(x,y,z,t)$. The vertical velocity of the bubble is extracted from a linear fit to the data $(z,t)$.

For the data reported in this paper, we use clean water from the Chemistry Department at Occidental College. The water is first taken from a deionized water source, which has been pretreated by a Culligan water purification system.[11] It is then distilled by an auto-distiller (Wheaton split-stream D-10N), and filtered by a 3-module filtration system (Nanopure, Barnstead). The surface tension $\sigma$ of the water is 72.8 dyn/cm at 21.8 °C measured with a Fisher Scientific tensiometer (Tensiomat Model 21). Experiments were also carried out using water from the Chemistry Department at Caltech, in which the water is filtered with a 4-module filtration system (Nanopure, Barnstead) with specific resistance of $\gtrsim 18\,\mathrm{M\Omega \cdot cm}$. Experimental results are consistent with the results presented below. Extreme caution is taken to keep the tank as clean as possible. Once the tank is filled with water, it is sealed immediately with plastic sheets. Air filters (VWR Scientific, 0.20 $\mu$m) are installed at all the air entrances to the experimental system. The temperature of the water during the experiment is 22±0.3 °C. To further ensure that our water is clean, we repeated the experiments of Duineveld[4] in our experimental setup; good agreements were obtained as discussed in the following paragraphs.

Initially, glass capillaries of different sizes were used for generating bubbles of different sizes. Surprisingly, we found that the inner diameter of the capillary $d_i$ played an important role in the shape and path of the air bubbles. In Fig. 2(a), the upper (cross) and lower (circle) data points are bubble velocities generated by the gentle-push method with capillary tube $d_i$=0.0267 cm and 0.120 cm, respectively. As seen,
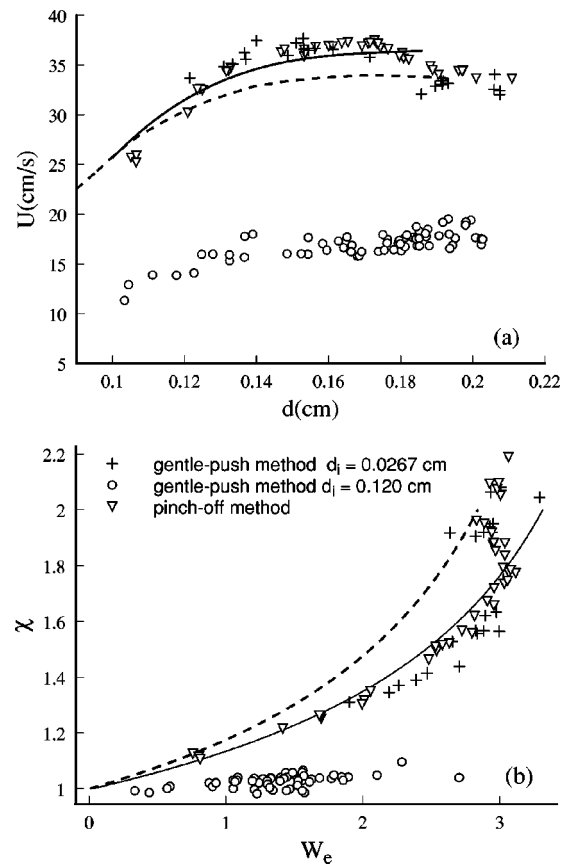
bubbles detached from small capillary rise nearly twice as fast as those from the large capillary. Three other capillary tubes of intermediate sizes, $d_i$=0.0376 cm, 0.0595 cm, and 0.0841 cm, have also been tested in our system. We found that bubbles generated by capillary tube of $d_i$=0.0376 cm followed the upper velocity curve and bubbles generated by the other two larger capillaries followed the lower velocity curve. To ensure that the purity of the water in the tank is not responsible for the difference between the two curves, we intentionally carry out experiments using the same batch of water. In Fig. 2(a), the lower (circle) and the upper (cross) curves are obtained consecutively using the same apparatus and water except for the capillary tubes, the lower curve being obtained first.

Images of bubbles at a position ~2.5 cm above the capillary tube were analyzed. The aspect ratio $\chi(\equiv a/b)$ versus Weber number We are shown in Fig. 2(b). Here, Weber number is defined as $\mathrm{We}\equiv 2\rho U^2/\sigma$, where $\rho$ is the density of the water. Figure 2(b) shows that the bubbles generated by the small capillary tube are mostly ellipsoidal in shape, with aspect ratios ranging from 1.1–2.2, while the bubbles generated by the large capillary tube are mostly spherical in shape, with aspect ratios ranging from 1.00–1.08.

To understand the effects of the size of capillary on the shape and motion of bubbles, we studied bubble images near the capillary tube. Figure 3 shows a series of images using
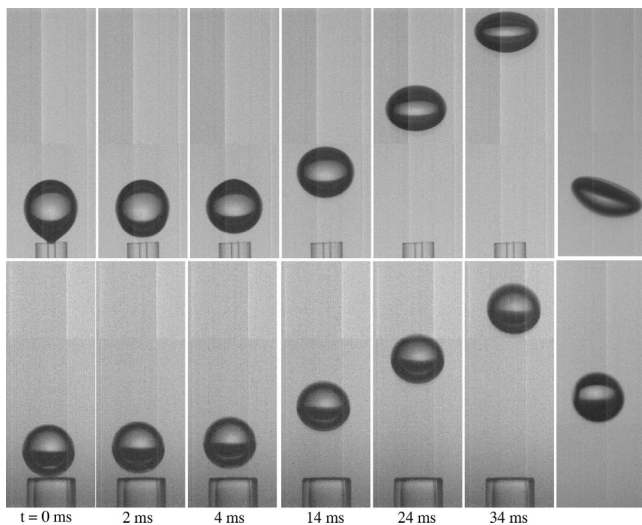
FIG. 3. Images of bubbles at detachment. The size of each image is 0.32 cm×0.88 cm. Bubbles are generated by the gentle-push method using capillary tube of $d_i=0.0267$ cm in the upper row, and $d_i=0.120$ cm in the lower row. The bubble diameter is 0.195 cm (0.188 cm) in the upper (lower) row. The right most image in the upper (lower) row is taken at ~6 cm (20 cm) above the capillary tip.

capillary tubes of two different inner diameters. In the upper row of images, the inner diameter of the capillary is 0.0267 cm, which is much smaller than the bubble diameter. The curvature at the bubble detachment point exhibits a local maximum. Such deformation gives rise to a strong axisym-

metric surface wave, which in turn propels the bubble to a large initial speed. In the lower row of images, the inner diameter of the capillary is 0.120 cm, which is similar to the bubble diameter. The bubble keeps its spherical shape due to the weak perturbations from the detachment process. By analyzing consecutive images in Fig. 3, we obtain a final vertical rising velocity of 18.5 cm/s at $t=20$ ms for the spherical bubble. An intermediate velocity of 30.0 cm/s is reached at $t=30$ ms for the ellipsoidal bubble, while its final velocity is 33.4 cm/s.

Figure 4 shows bubble trajectories for spherical and ellipsoidal bubbles of various bubble diameters. For ellipsoidal bubbles, a straight path of the bubble switches to a spiral path [see rows (a) and (b) of Fig. 4] when the bubble diameter exceeds ~0.15 cm or aspect ratio exceeds ~1.6. For nearly spherical bubbles, the straight path of the bubble switches to a zigzag path [see rows (c) and (d) of Fig. 4] when the bubble diameter exceeds ~0.15 cm or Reynolds number exceeds ~280. The details of the transitions are being investigated and will be reported in a later publication.

One interesting observation is the resemblance between the zigzagging instabilities of spherical bubbles and vortex shedding phenomena in the wake of a solid sphere. For rising air bubbles, we find that the critical Reynolds number for path instability is $R_{ec}=275\pm25$, and Strouhal number St $=0.087\pm0.003$, drag coefficient $C_D=0.80\pm0.06$ at $R_e=300$. For the wake of a solid sphere, it is reported that $R_{ec}$ for vortex shedding is 280, and St$=0.12$, $C_D=0.65$ at $R_e$
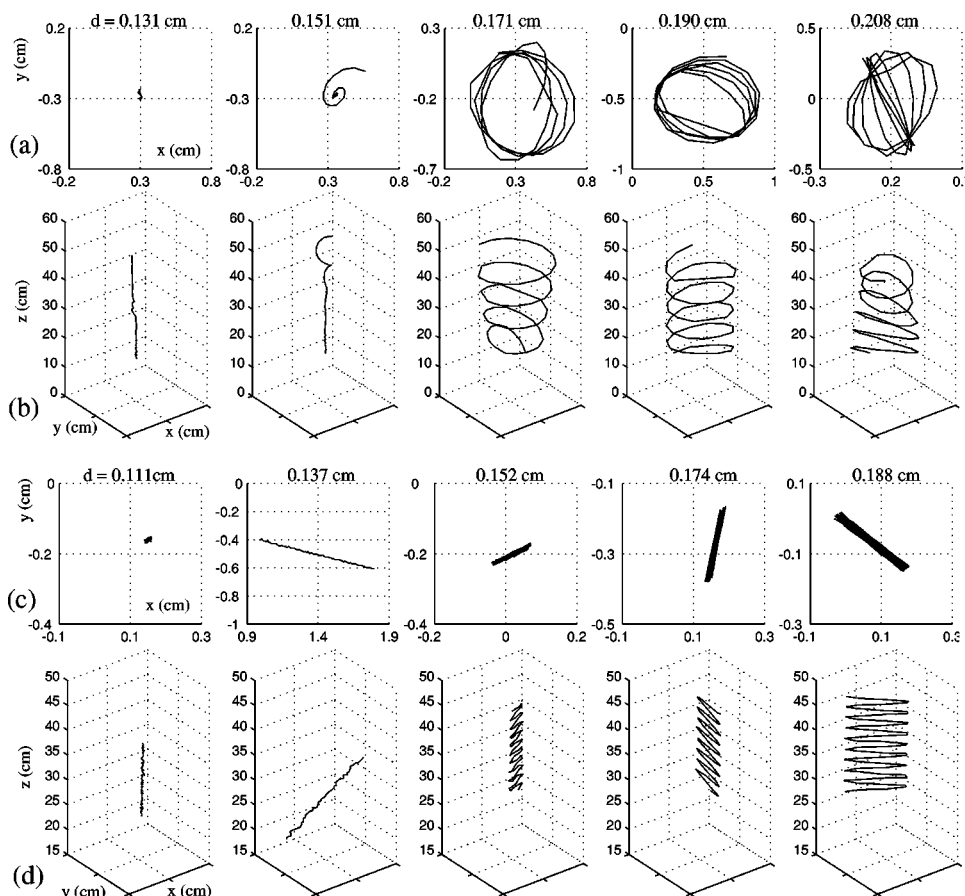


FIG. 4. Row a (c): Top view of the measured spiral (zigzag) trajectories. Row b (d): 3D rendition of the spiral (zigzag) trajectories. The diameter of the bubble $d$ is labeled on each 2D plot.

=300.[1,12] It should be noted that a fair comparison should be made between freely rising air bubbles and freely rising solid spheres. However, it is known that freely rising spheres do not exhibit a clear transition from a straight path to a regular zigzag path.[13]

We repeated our experiments using a second generation method which we call the pinch-off method. This method has been used frequently in previous investigations.[5,6,9,13] In this method, air comes from a syringe and goes directly to the hypodermic needle located at the bottom of the tank. The bubble detaches naturally from the needle due to the buoyancy force. The bubble size depends on the needle size as well as the shape of the needle tip. For the bubble to detach naturally from the needle, the inner diameter of the needle $d_i$ needs to be much smaller than the bubble diameter $d$. In our case, $d_i$ ranges from 0.031–0.044 cm. The shape and path of the bubbles generated by the pinch-off method are similar to those generated by the gentle-push method with capillary $d_i=0.0267$ cm (shown as triangle data points in Fig. 2).

In summary, we find that bubbles (diameter range of 0.1–0.2 cm) rising in clean water retain an ellipsoidal shape when they detach from a small capillary tube ($d_i\leqslant0.0376$) and retain a spherical shape when they detach from a large capillary tube ($d_i\geqslant0.0595$ cm). The ellipsoidal bubbles exhibit a spiralling path instability, while the spherical bubbles exhibit a zigzagging path instability when the bubble diameter exceeds ～0.15 cm.

While ellipsoidal bubbles rising in clean water have been studied extensively by many authors[4–6,9] and have been understood within the theoretical framework of Moore,[14] the intriguing question arising from the above observations is the appearance of spherical bubbles in clean water. Currently, no analytical theory and numerical simulations support the existence of spherical clean bubbles, and previous experiment shows that only contaminated bubbles can be spherical in this diameter range.[15] From an experimental point of view, both ellipsoidal and spherical bubbles in our experiments are likely to possess the same cleanness at point of detachment because these bubbles are generated in the same apparatus (except for the capillary tubes) and in the same batch of water. However, ellipsoidal bubbles follow the behavior of clean bubbles, while spherical bubbles exhibit behavior close to, but not exactly the same as, that of contaminated bubbles. Since we do not have direct knowledge of whether the bubble surface is free from contaminants, we are left with two possible choices. The spherical bubbles can be either clean or contaminated. If the spherical bubbles are clean, then the ellipsoidal and spherical bubbles are two stable solutions to the problem. As mentioned above, there is no analytical or numerical work to support this possibility at present. The other explanation, suggested by Prosperetti, is that the steady ellipsoidal bubbles are clean and the steady spherical bubbles are contaminated. In this scenario, both types of bubbles are contaminated at the point of detachment when passing through the bubble generation apparatus. However, the shape oscillations that occur right after the detach-

ment from the small capillary tube may be strong enough to clean the bubble surface. In our purified water, recontamination is then so slow that the bubble remains clean over the duration of the experiment. If this is indeed the case, such surface oscillations may provide a new technique for making small clean bubbles.

These experimental results also shed light on some of the inconsistencies in the literature. Saffman used a gentle-push method in which capillaries of inner diameter of 0.08 cm and 0.16 cm were used,[7] and only zigzagging bubbles were observed. On the other hand, Miyagi[5] and Aybers and Tapucu[9] used a pinch-off method, and only spiralling bubbles were observed. It should be noted that such correspondence between the size of the capillary tube and the bubble trajectory only applies to bubbles in the diameter regime of 0.1–0.2 cm and rising in treated water.

## ACKNOWLEDGMENT

[1] R. Clift, J. R. Grace, and M. E. Weber, *Bubbles, Drops and Particles* (Academic, New York, 1978).

[2] J. Magnaudet and I. Eames, "The motion of high-Reynolds-number bubbles in inhomogeneous flows," Annu. Rev. Fluid Mech. **32**, 659 (2000).

[3] G. K. Batchelor, *An Introduction to Fluid Dynamics* (Cambridge University Press, Cambridge, 1967).

[4] P. C. Duineveld, "The rise velocity and shape of bubbles in pure water at high Reynolds number," J. Fluid Mech. **292**, 325 (1995).

[5] O. Miyagi, "The motion of air bubbles rising in water," Technol. Rep. Tohoku Univ. **5**, 135 (1925).

[6] W. L. Haberman and R. K. Morton, "An experimental investigation of the drag and shape of air bubbles rising in various fluids," David Taylor Model Basin Report 802, 1953.

[7] P. G. Saffman, "On the rise of small air bubbles in water," J. Fluid Mech. **1**, 249 (1956).

[8] R. A. Hartunian and W. R. Sears, "On the instability of small gas bubbles moving uniformly in various liquids," J. Fluid Mech. **3**, 27 (1957).

[9] N. M. Aybers and A. Tapucu, "The motion of gas bubbles rising through stagnant liquid," Waerme- Stoffuebertrag. **2**, 118 (1969).

[10] C. E. Willert and M. Gharib, "Three-dimensional particle imaging with a single camera," Exp. Fluids **12**, 353 (1992).

[11] The Culligan water purification system consists of one carbon filter, two 0.45 $\mu$m filters, one reverse osmosis system, two deionization columns, one ultraviolet water sterilizer and two 0.22 $\mu$m filters. The specific resistance of the water is 10 M$\Omega \cdot$cm.

[12] D. Ormiéres and M. Provansal, "Transition to turbulence in the wake of a sphere," Phys. Rev. Lett. **83**, 80 (1999).

[13] K. Lunde and R. J. Perkins, "Observations on wakes behind spheroidal bubbles and particles," ASME-FED Summer Meeting, Vancouver, Canada, 1997, paper number FEDSM97-3530.

[14] D. W. Moore, "The velocity of rise of distorted gas bubbles in a liquid of small viscosity," J. Fluid Mech. **23**, 749 (1965).

[15] R. Bel Fdhila and P. C. Duineveld, "The effect of surfactant on the rise of a spherical bubble at high Reynolds and Peclet numbers," Phys. Fluids **8**, 310 (1996).